J. Appl. Comput. Mech., 7(2) (2021) 396-403
DOI: 10.22055/JACM.2020.34734.2468

ISSN: 2383-4536
jacm.scu.ac.ir

Journal of
Applied and Computational Mechanics

Research Paper

Multiscale Numerical Modeling of Solute Transport with Two-Phase Flow in a Porous Cavity

Mohamed F. El-Amin, Shereen Abbdel-Naeem

Mathematics Department, Faculty of Science, Aswan University, Aswan 81528, Egypt

Received August 23 2020; Revised September 15 2020; Accepted for publication September 15 2020.
Corresponding author: Mohamed F. El-Amin (mfam2000@yahoo.com)

Abstract. This paper introduces dimensional and numerical investigation of the problem of solute transport within the two-phase flow in a porous cavity. The model consists of momentum equations (Darcy's law), mass (saturation) equation, and solute transport equation. The cavity boundaries are constituted by mixed Dirichlet-Neumann boundary conditions. The governing equations have been converted into a dimensionless form such that a group of dimensionless physical numbers appear including Lewis, Reynolds, Bond, capillary, and Darcy numbers. A time-splitting multiscale scheme has been developed to treat the time derivative discretization. Also, we use the Courant-Friedrichs-Lewy (CFL) stability condition to adapt the time step size. The pressure is calculated implicitly by coupling Darcy's law and the continuity equation, then, the concentration equation is solved implicitly. Numerical experiments have been conducted and the effects of the dimensionless numbers have been on the saturation, concentration, pressure, velocity, and Sherwood number have been investigated.

Keywords: Porous cavity; Solute transport; Two-phase flow; Time-splitting; Multiscale.

1. Introduction

The topic of solute transport in porous media has many applications such as environment, geophysics and petroleum/chemical engineering. For example, solute transport with fluid flow in porous media are commonly used in tracer transport tests to check the interconnectivity of production wells in oil reservoirs. Also, the contaminant transport in underground due to chemical wastes storages is extremely important in environmental applications. In order to understand the behavior of solute transport in underground, the mathematical modeling and simulation is the best way to do handle it. The modeling of solute transport through porous media has been built based on continuum theory to derive the governing differential equations. There are different approaches to model solute transport in porous media such as Markov theory of kinematic approache with statistical thermodynamics and continuum mechanics approache [1]. The solute transport model has been solved using different approach from analytical solutions (e.g. [2, 3]) to numerical solutions (e.g. [4, 21, 22]). In fact, there are a large number of research papers that tackle solute transport physics in porous media and its heterogeneity [23] and diverse applications [24, 25]. However, to obtain an analytical solution, the model is usually simplified, which causes that the model loses some of its functionality to describe the physical phenomenon correctly. So, it was worthy to looking for numerical solutions that are able to provide full simulation of the physical problem under consideration. On the other hand, a numerical solution has its own difficulties which one needs to overcome and develops the robust numerical methods. There are two key numerical techniques that treat the temporal discretization in the problems of flow and transport in porous media, including the IMplicit Pressure Explicit Saturation (IMPES) method, and the fully-implicit one. The IMPES method is much faster than the fully implicit method, however, it has less stability due to the explicit treatment of the capillary pressure term and mobility coefficients. On the other hand, the fully-implicit scheme takes so much time, but is unconditionally stable. The IMPES scheme solves the pressure equation implicitly, while treats the saturation equation explicitly. Some researchers [5-8] expanded the IMPES method to treat more implicit equations such as the solute and/or heat equation. Also, significant improvements are added to the IMPES methods such as the research work in Refs. [9-12, 20]. The time-splitting multiscale strategies have been used with IMPES method and its different versions and other extensions as well [13-18, 27].

The square (porous) cavity is usually used as a benchmark geometry to test fluid flow and heat/mass transfer numerical problems. A significant amount of research work has been done in literature to investigate the heat transfer behavior in in a porous cavity [28]-[32]. For example, El-Amin and Abbdel-Naeem [26] developed a numerical technique to solve the problem of nonisothermal two-Phase flow in a porous cavity. Also, El-Amin et al. [33] studied the effects of magnetic field on ferromagnetic fluids associated with heat transfer in a porous cavity.

In the current work, we use the approach of continuum mechanics to develop governing differential equations. The governing equations which describe the solute transport with two-phase flow in porous media has been provided, then transformed into a dimensionless form. The non-dimensional equations include several physical numbers such as Lewis, Reynolds, Bond, capillary and Darcy numbers. We develop an adaptive time-splitting scheme to be combined with IMPES and Implicit concentration (i.e., IMPCES) algorithm to solve the problem under consideration. The cell-centered finite difference (CCFD) method has been used for

Published online: September 16 2020

the spatial discretization [19]. The CFL stability condition has been used to achieve the adaptivity of the time step-size. The effects of Lewis, Reynolds, Bond, capillary and Darcy number on the local Sherwood, concentration, velocity, pressure and saturation are discussed in the results.

2. Analysis

Referring to the sketch of the problem in Fig. 1, one may notice that all the cavity walls are kept at low concentration, C_c, except the inlet is kept at high concentration, C_h.

The problem of two-phase fluids flow in heterogeneous porous media is presented in this section. The two fluids are assumed to be incompressible and immiscible. The model which governs the physical phenomena is given by the conservation laws of momentum and mass (saturation equation). Thus, the momentum equation is represented by Darcy's law with Boussinesq approximation as,

$$\mathbf{u_\alpha} = -\frac{k_{r\alpha}}{\mu_\alpha}\mathbf{K}\left(\nabla p_\alpha + g\rho_\alpha\left(1-\beta^*(C-C_c)\right)\right),\ \ \alpha = w,n \tag{1}$$

In the Boussinesq approximation, the density is given by,

$$\rho_\alpha = \rho_\alpha\left(1-\beta^*(C-C_c)\right),\quad \alpha = w,n$$

such that β^* is the expansion coefficient which is given by,

$$\beta^* = -\frac{1}{\rho_{\alpha,0}}\frac{\partial \rho_\alpha}{\partial c},\ \ \alpha = w,n$$

The continuity (mass-conservation) equation of the two-phase is represented by the two saturation equations,

$$\varphi\frac{\partial s_\alpha}{\partial t} + \nabla\cdot\mathbf{u_\alpha} = q_\alpha,\ \ \alpha = w,n \tag{2}$$

Assuming that the solute exists only the wetting phase, the solute transport equation can be written in the form,

$$\varphi\frac{\partial (s_w c)}{\partial t} + \nabla\cdot(\mathbf{u}_w c - D\nabla c) = q_c \tag{3}$$

The summation of the saturation of the two phases is one, thus,

$$\sum_\alpha s_\alpha = 1,\ \ \alpha = w,n$$

where $\varphi[-], \mathbf{u_\alpha}$ [m/s] and ρ_α [Kg/m^3], $s_\alpha[-]$ are, respectively, the porosity, velocity, fluid density, and saturation of the phase α. The wetting phase is denoted by w, and the nonwetting one by nw, while s refers to the solid. Q_t[m^3/s], $\mathbf{K}$ and g are the heat source term, the permeability and the gravitation acceleration, respectively. $p_\alpha, k_{r\alpha}, \mu_\alpha$ refer to the pressure, relative permeability, and viscosity, respectively. q_α and q_c are the external source/sink terms.

3. Dimensionless Analysis

The following non-dimensional variables are presented,

$$(U,V) = \frac{(u,v)}{v},\ (U_w,V_w) = \frac{(u_w,v_w)}{v},\ (X,Y) = \frac{(x,y)}{H},\ \tau = \frac{vt}{\varphi H^2},\ \emptyset = \frac{C-C_c}{C_h-C_c},\ S = \frac{s_w - s_{iw}}{1-s_{rnw}-s_{iw}} \tag{4}$$

s_{iw} is the irreducible saturation and s_{rnw} is the residual saturation of the nonwetting phase, such that, $0 \le S \le 1$. Therefore, the capillary pressure and its gradient can be expressed as,

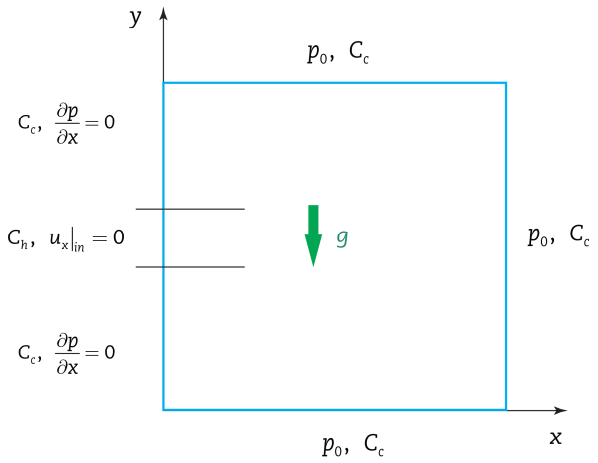

Fig. 1. Schematic diagrams of the 2D square porous cavity.

$$p_c = \gamma \left(\frac{\varphi}{k}\right)^{\frac{1}{2}} J(S),\ \nabla p_c = \frac{\gamma}{H}\left(\frac{\varphi}{k}\right)^{\frac{1}{2}} \frac{dJ(S)}{dS} \nabla S \tag{5}$$

Now, let us use the following nondimensional physical parameters,

$$Da^{1/2} = \frac{k^{1/2}}{H},\ Re_w = \frac{U_w H}{\upsilon},\ Le = \frac{\alpha}{D},\ Bo = \frac{\Delta \rho_\alpha g H^2}{\gamma},\ ca_w = \frac{\mu_w U_w}{\gamma},\ Da = \frac{k}{H^2}$$

where ca_w is the capillary number, Da is the Darcy number, Re_w is the Reynolds number, Le is the Lewis number, and Bo is the Bond number.

The governing eqs. (1) – (3) become in the dimensionless form as follows:

Saturation equation,

$$\frac{\partial S}{\partial \tau} + \frac{Da^{1/2}.\ Re}{ca_w} \psi \nabla \cdot \left\{ \frac{k_{rw}^o s^a m_{nwo}(1-s)^b}{m_{wo} s^a + m_{nwo}(1-s)^b} \left[\varphi^{\frac{1}{2}} \frac{dJ(S)}{dS} \nabla S - Da^{1/2}\, Bo \right] \right\} = Q_w \tag{6}$$

Concentration equation,

$$\frac{\partial (Sm + s_{iw})\emptyset}{\partial \tau} + \nabla \cdot (U_w \emptyset - \frac{1}{Le} \nabla \emptyset) = Q_c \tag{7}$$

where

$$m = (1 - s_{rnw} - s_{iw}),\ Q_w = \frac{H^2}{\upsilon m} q_w,\ \psi = \frac{1}{m},\ Q_c = \frac{H^2}{\upsilon (C_h - C_c)} q_c,\ m_w = \frac{k_{rw}}{\mu_w},\ m_{nw} = \frac{k_{rnw}}{\mu n_w},\ m_w = m_{wo} s^a,\ m_{nw} = m_{nwo}(1-s)^b, m_{wo} = \frac{k_{rw}^o}{\mu_w}.$$

The boundary conditions in dimensionless form become,

Left wall: $\emptyset_{in} = 1,\ U = U_{in},\ X = 0,\ 0 \le Y \le 1,\ \emptyset = 0,\ \frac{\partial P}{\partial X} = 0$

Bottom wall: $0 \le X \le 1,\ Y = 0,\ \Theta = 0, \emptyset = 0,\ P = P_0$

Right wall: $X = 1,\ 0 \le Y \le 1,\quad \Theta = 0,\ \emptyset = 0,\ P = P_0$

Top wall: $0 \le X \le 1,\ Y = 1,\ \Theta = 0,\ \emptyset = 0,\ P = P_0$

In eq. (2), adding the saturation equation for the two-phase (wetting and nonwetting), the pressure equation given as,

$$\nabla \cdot \boldsymbol{U}_t = -\nabla \cdot m_t \boldsymbol{K} \nabla (p_w + g \rho_\alpha (1 - \beta^* (C - C_c)) - \nabla \cdot m_n \boldsymbol{K} \nabla (p_c + g \Delta \rho_\alpha (1 - \beta^* (C - C_c))) = q_t \tag{8}$$

where $\mathbf{U}_\mathrm{t} = \mathbf{U}_\mathrm{w} + \mathbf{U}_\mathrm{n}$ is the total velocity, $p_c(S) = p_n - p_w$ is the capillary pressure, $q_t = q_w + q_n$ is the total source mass transfer, $\Delta\rho = \rho_n - \rho_w,\ f_w = \frac{m_w}{m_t}$ is the flow fraction, $m_t = \frac{k_{r\alpha}}{\mu_\alpha}$ is the phase mobility, and $m_t = m_w + m_n$ is the total mobility.

Adding eq. (6) to eq. (2) gives the water pressure equation as,

$$\frac{\partial S}{\partial \tau} - Q_w = -\nabla \cdot \lambda_w \boldsymbol{K} \nabla \left(p_w + g \rho_\alpha (1 - \beta^* (C - C_c)) \right) \tag{9}$$

where $\lambda_w = \frac{H^2 m_w}{\upsilon (1 - s_{rnw} - s_{iw})}$.

Hence the saturation equation can be updated by the following,

$$\frac{\partial S}{\partial \tau} - Q_w = -\nabla \cdot (f_w \mathbf{U}_\mathrm{a}) \tag{10}$$

where $\mathbf{U}_w = f_w \mathbf{U}_\mathrm{a} = -\nabla \cdot \lambda_w \boldsymbol{K} \nabla (p_w + g \rho_\alpha (1 - \beta^* (C - C_c)))$.

The capillary pressure has been given by the formula, $p_c = -p_d \log S$, is the normalized saturation, p_d is the entry pressure. The relative permeabilities are given as, $k_{rw} = k_{rw}^0 s_w^2,\ k_{rn} = k_{rn}^0 (1 - s_w)^2$, such that, $k_{rw}^0 = k_{rw}(s_w = 1)$, and $k_{rn}^0 = k_{rn}(s_w = 1)$.

The diffusion-dispersion tensor is given by,

$$D = \varphi s_w \tau (D^{Br} + D^{disp}) \tag{11}$$

where τ is the tortuosity parameter of the water phase. Br is the diffusion of Brownian. D^{disp} is the coefficient of dispersion which is given by,

$$\varphi s_w \tau D^{disp} = d_{t,w} |\boldsymbol{u}_w| \boldsymbol{I} + (d_{l,w} - d_{t,w}) \frac{\boldsymbol{u}_w \boldsymbol{u}_w^T}{|\boldsymbol{u}_w|} \tag{12}$$

Thus,

$$D = \left(\varphi s_w \tau D^{Br} + d_{t,w}|\boldsymbol{u}_w|\right)\boldsymbol{I} + (d_{l,w} - d_{t,w})\frac{\boldsymbol{u}_w \boldsymbol{u}_w^T}{|\boldsymbol{u}_w|} \tag{13}$$

where $d_{l,w}$ and $d_{t,w}$ are the dispersion coefficients.

The local surface mass fluxes, j_x, j_y may be given by,

$$j_x = -D\frac{\partial C}{\partial X}\Big|_{X=0}, \quad j_y = -D\frac{\partial C}{\partial Y}\Big|_{Y=0} \tag{14}$$

Therefore, the local Sherwood number becomes,

$$Sh_X = \frac{j_x L_x}{(C_w - C_0)k} = -\frac{1}{(C_w - C_0)}\frac{\partial \emptyset}{\partial X}\Big|_{X=0}, \quad Sh_Y = \frac{j_y L_y}{(C_w - C_0)k} = -\frac{1}{(C_w - C_0)}\frac{\partial \emptyset}{\partial Y}\Big|_{Y=0} \tag{15}$$

4. Numerical Method

The time-splitting method splits the time interval into some subintervals based on how fast the variation in physics, thus, the pressure equation has bigger time-step size than the time-step size of saturation and concentration. Therefore, the outer time interval, [0, T], of pressure is divided into a number of N_p time-steps, i.e., $0 = t_0 < t_1 < \cdots < t_{N_p=T}$, $\Delta t^k = t^{k+1} - t^k$. Then, each outer interval, (t^k, t^{k+1}), is divided into $N_{p,s}$ subintervals to suite saturation variation, i.e., $(t^k, t^{k+1}) = \cup_{l=0}^{N_{p,s}-1}(t^{k,l}, t^{k,l+1})$. The upper level of time discretization is for concentration because its variation is faster than saturation. So, each subinterval $(t^{k,l}, t^{k,l+1})$ can be partitioned into $N_{p,s,c}$ subsubintervals as, $(t^{k,l}, t^{k,l+1}) = \cup_{m=0}^{N_{p,s,c}-1}(t^{k,l,m}, t^{k,l,m+1})$. It is noteworthy that the initial time-step of saturation is taken same as of the pressure, i.e., $\Delta t^{k,0} = \Delta t^k$, and the initial time-step of concentration is the same as the one of saturation, i.e., $\Delta t^{k,l,0} = \Delta t^{k,l}$. If $\mathrm{CFL}_{C,X} > 1$ or $\mathrm{CFL}_{C,Y} > 1$, the concentration time-step will be divided into smaller steps, then, $\mathrm{CFL}_{C,X}$ and $\mathrm{CFL}_{C,Y}$ will be recalculated based on the new time-step and so on until reach $\mathrm{CFL}_{C,X} < 1$ and $\mathrm{CFL}_{C,Y} < 1$. Similar technique can be used for saturation time-step adaptation using $\mathrm{CFL}_{S,Y}$ and $\mathrm{CFL}_{S,Y}$.

For the time-derivative of the equations of concentration, the backward Euler time discretization has been used [9, 14, 20, 27]. Also, we linearize the function of the capillary pressure by saturation, i.e.,

$$p_c(s_w^*) \cong p_c(s_w^k) + p_c'(s_w^k)[s_w^{k+1} - s_w^k] \tag{16}$$

which can be written as,

$$p_c(mS^* + s_{iw}) \cong p_c(mS + s_{iw})^k + p_c'(mS + s_{iw})^k[(mS + s_{iw})^{k+1} - (mS + s_{iw})^k] \tag{17}$$

where p_c' is the derivative of p_c. The quantity, $[(mS + s_{iw})^{k+1} - (mS + s_{iw})^k]$, can be calculated from the saturation equation as,

$$[(mS + s_{iw})^{k+1} - (mS + s_{iw})^k] = \Delta\tau^k\left[Q_w^{k+1} - \nabla \cdot \lambda_w(S^k)\boldsymbol{K}\nabla\left(p_w^{k+1} + g\rho_w\left(1 - \beta^*(C^{k+1} - C_c)\right)\right)\right] \tag{18}$$

Therefore, the pressure equation becomes,

$$-\nabla \cdot \lambda_t(S^k)\boldsymbol{K}\nabla(p_w^{k+1} + g\rho_w\left(1 - \beta^*(C^{k+1} - C_c)\right) - \nabla \cdot \lambda_n(S^k)\boldsymbol{K}\nabla(p_c(S^*) + g\rho_w\left(1 - \beta^*(C^{k+1} - C_c)\right)) = q_t^{k+1} \tag{19}$$

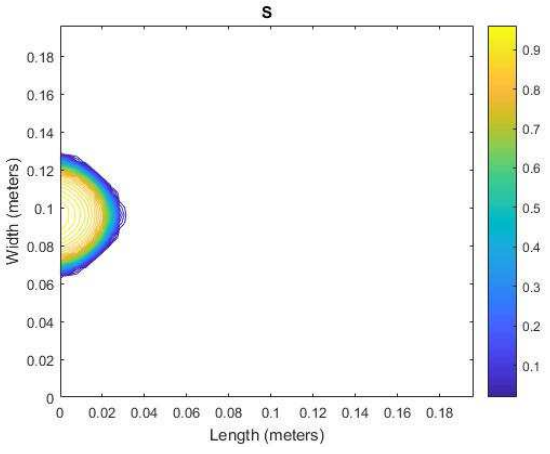

Fig. 2. Saturation distribution for Le=0.3, $Da^{0.5}\, Re/ca_w = 1$ and $Da^{0.5}\, Bo = 0.00001$.

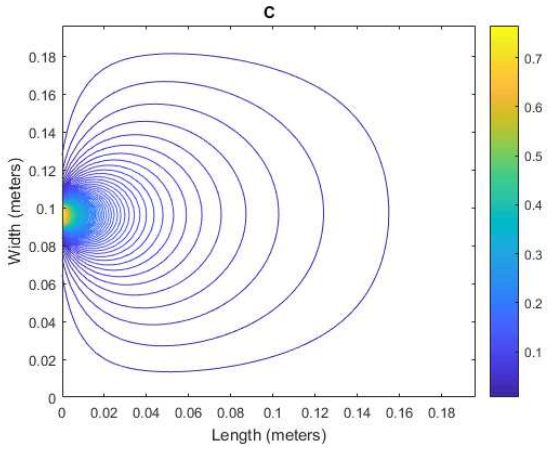

Fig. 3. Concentration distribution for Le=0.3, $Da^{0.5}\, Re/ca_w = 1$ and $Da^{0.5}\, Bo = 0.00001$.

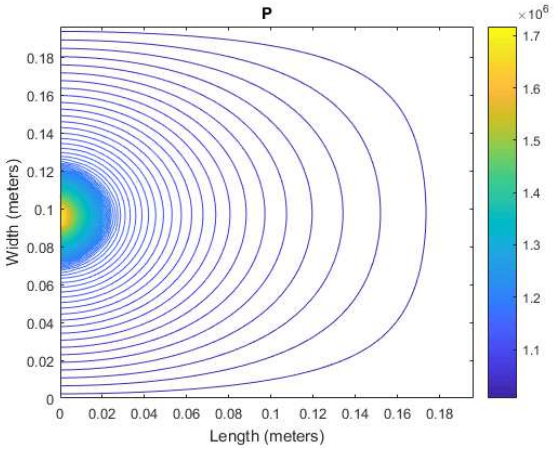

Fig. 4. Pressure distribution for Le=0.3, $Da^{0.5}\,Re/ca_w = 1$ and $Da^{0.5}\,Bo = 0.00001$.

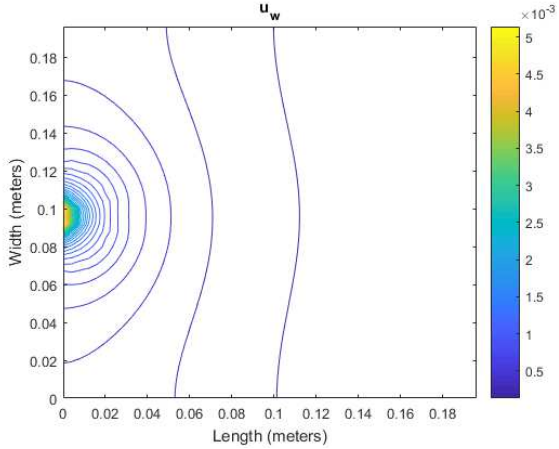

Fig. 5. Velocity distribution for Le=0.3, $Da^{0.5}\,Re/ca_w = 1$ and $Da^{0.5}\,Bo = 0.00001$.

The water pressure p_w is obtained by solving the coupled system (17)-(19) implicitly. Then, the saturation is obtained explicitly using,

$$\frac{S^{k,l+1}-S^{k,l}}{\Delta\tau^l} + \nabla.(f_w^k \boldsymbol{U}_a^{k+1}) = Q_w{}^{k,l+1} \tag{20}$$

The concentration equation is computed implicitly as,

$$\frac{S^{k+1}\emptyset^{k,l,m+1}\beta - S^k\emptyset^{k,l,m}\beta}{\Delta\tau^m} + \nabla\cdot(\boldsymbol{U}_w{}^{\boldsymbol{k+1}}\emptyset^{k,l,m+1} - \frac{1}{Le}\nabla\emptyset^{k,l,m+1}) = Q_c{}^{k,l,m+1} \tag{21}$$

The Courant-Friedrichs-Lewy (CFL) stability condition is utilized here to adapt the time-step size for each physical variable by holding CFL<1. The CFLs for the saturation equations in dimensionless form are,

$$CFL_{S,X} = H\varphi\frac{\boldsymbol{U}_X\Delta\tau^{k,l}}{\Delta X}, \quad CFL_{S,Y} = H\varphi\frac{\boldsymbol{U}_Y\Delta\tau^{k,l}}{\Delta Y} \tag{22}$$

The concentration equation in dimensionless form are given by,

$$CFL_{C,X} = H\varphi\frac{\boldsymbol{U}_X\Delta\tau^{k,l,m}}{\Delta X}, \quad CFL_{C,Y} = H\varphi\frac{\boldsymbol{U}_Y\Delta\tau^{k,l,m}}{\Delta Y} \tag{23}$$

5. Results and Discussions

In Table 1, we provid error estimations for the numerical solutions, namely, saturation and concentration with different given outer time-step number k. The reference solutions were calculated at a single point in the domain after 2000 time step. It is clear that decreases as number k increases.

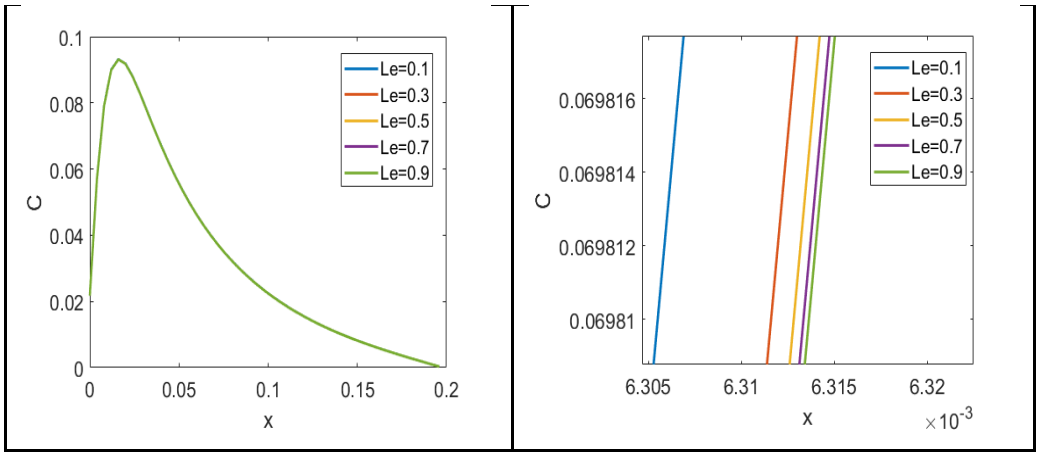

Fig. 6. Effects of Lewis number (Le=0.1, 0.3, 0.5, 0.7, 0.9) on the concentration at $Da^{0.5}\,Re/ca_w = 1$ and $Da^{0.5}\,Bo = 0.00001$.

Table 1. Error estimation of saturation and concentration for different number of time steps k.

k	$\|S^{n+1,k+1} - S_r^n\|$	$\|C^{n+1,k+1} - C_r^n\|$
100	0.0191	0.0088
200	0.0160	0.0056
500	0.0148	0.0024
800	0.0109	0.0018

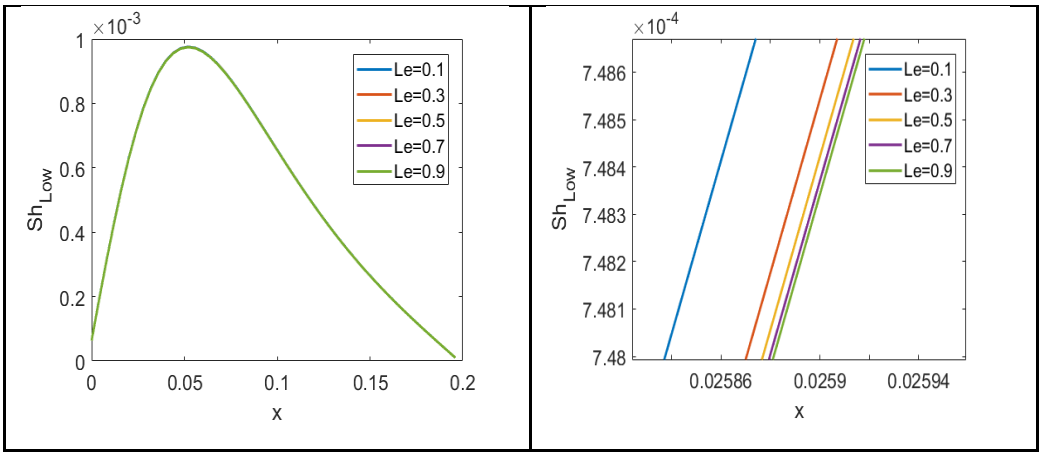

Fig. 7. Effects of Lewis number (Le=0.1, 0.3, 0.5, 0.7, 0.9) on the local Sherwood number at $Da^{0.5}\, Re/ca_w = 1$ and $Da^{0.5}\, Bo = 0.00001$.

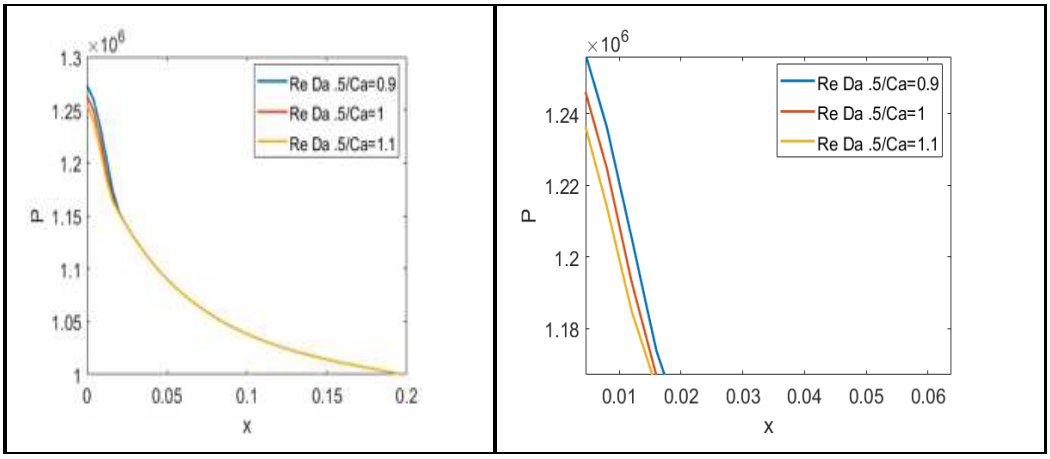

Fig. 8. Effects of $Da^{0.5}\, Re/ca_w$ on the pressure at Le=0.3 and $Da^{0.5}\, Bo = 0.00001$.

A square cavity of dimension 1×1 m is discretized into 20×20 rectangular cells have been used to obtain some numerical tests for the problem under investigation. The results of concentration, velocity, pressure, saturation, and local Sherwood number under the effects of Lewis number, and the two dimensionless coefficients $Da^{0.5}\, Re/ca_w$ and $Da^{0.5}\, Bo$ have been calculated and presented in graphs. The range of the parameters are $0.1 \leq$ Le ≤ 0.9, $0.9 \leq Da^{0.5}\, Re/ca_w \leq 1.1$ and $0.00001 \leq Da^{0.5}\, Bo \leq 0.1$. The contours of saturation, concentration, pressure and velocity are presented in Figs. 2-5, respectively. As shown in Fig. 2, the saturation distribution is high around the inlet region and gradually decreases as it gets farther. Concentration profiles in the square cavity are plotted in Fig. 3. From this figure, it can be seen that there is a reduction in concentration everywhere but it is still high at the inlet region, thus, the concentration decreases gradually from the inlet location to the far-field. The pressure distribution is plotted in Fig. 4. The pressure is high close to the inlet and decreases gradually from as it gets farther. The velocity distribution has been plotted in Fig. 5 which shows that the maximum value of velocity occurs along the central portion of the left wall where the inlet exists and decreases as we move away from the inlet.

Figures 6 and 7 depicts the influences of Lewis number (Le) on the concentration and local Sherwood number for $Da^{0.5}\, Re/ca_w = 1$ and $Da^{0.5}\, Bo = 0.00001$ for different Lewis number (Le=0.1, 0.3, 0.5, 0.7, 0.9). It can be seen that with Le increasing, the concentration and local Sherwood number increase. The effects of the parameter, $Da^{0.5}\, Re/ca_w$, on the pressure, concentration, and velocity are demonstrated in Figs. 8 – 10, respectively, for Le=0.3, $Da^{0.5}\, Bo = 0.00001$ with different $Da^{0.5}\, Re/ca_w$ (= 0.9, 1, 1.1). It can be observed from these figures that the concentration and pressure increase while $Da^{0.5}\, Re/ca_w$ decreases, but the velocity increases as $Da^{0.5}\, Re/ca_w$ increases. The effects of the parameter, $Da^{0.5}\, Bo$ on the pressure are demonstrated in Fig. 11 for Le=0.3 and $Da^{0.5}\, Re/ca_w = 1$ with $Da^{0.5}\, Bo = 0.00001,\ 0.001, 0.1$. It can be observed that the pressure decreases while $Da^{0.5}\, Bo$ increases.

6. Conclusion

In the present work, the problem of solute transport with two-phase flow in a porous cavity into has been investigated. First, the model of the problem under consideration has been developed. Second, we developed a group of transformations to transform governing equations into dimensionless form. The nondimensional governing equations are solved numerically using adaptive multiscale time-stepping scheme. The multiscale scheme is mainly managed by evaluating CFL conditions ($CFL_{S,X}$, $CFL_{S,Y}$, $CFL_{C,X}$, $CFL_{C,Y}$) and satisfy CFL< 1 at each sup-step to adapt the time-step size for each physics. The CCFD method has been used to discretize the governing equations. Some numerical experiments have been presented to test the effects of Lewis, Reynolds, Bond, capillary and Darcy number on temperature, concentration, pressure, velocity, saturation, and local Sherwood number.

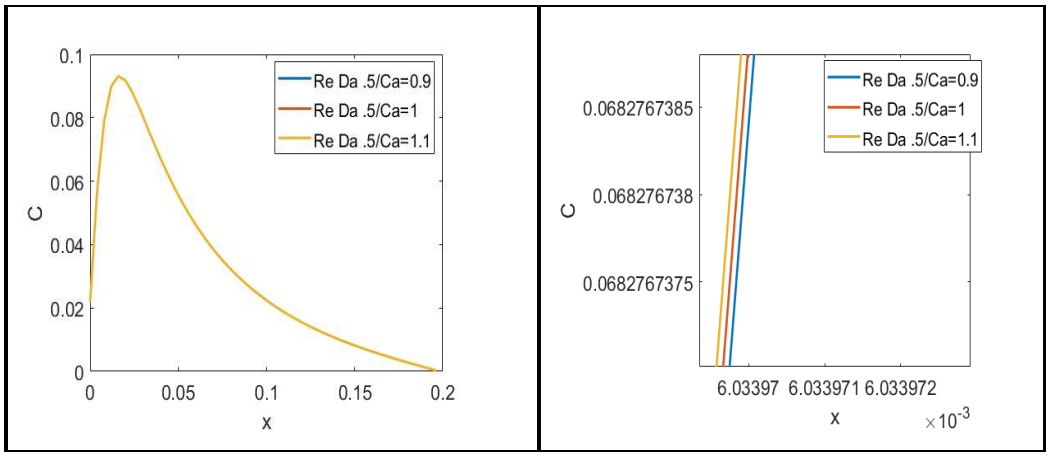

Fig. 9. Effects of $Da^{0.5}\, Re/ca_w$ on the concentration at Le=0.3 and $Da^{0.5}\, Bo = 0.00001$.

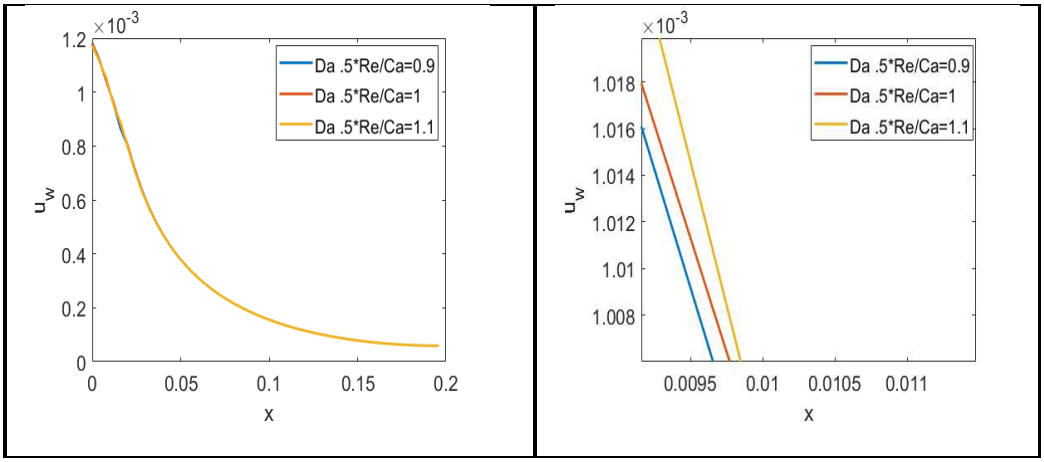

Fig. 10. Effects of $Da^{0.5}\, Re/ca_w$ on the velocity at Le=0.3 and $Da^{0.5}\, Bo = 0.00001$.

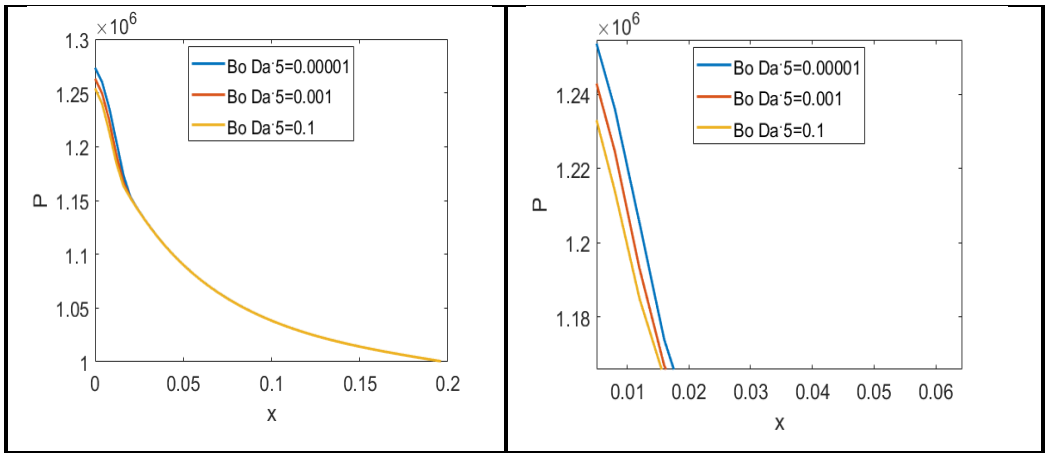

Fig. 11. Effects of $Da^{0.5}\, Bo$ on the pressure at Le=0.3 and $Da^{0.5}\, Re/ca_w = 1$.

Author Contributions

M.F. El-Amin planned the research, developed the mathematical modeling and examined the theory validation, initiated the coding, and suggested the methodology; S.M. Abdel-Naeem running the code and analyzed the results. The manuscript was written through the contribution of the two authors. The two authors discussed the results, reviewed, and approved the final version of the manuscript.

Conflict of Interest

The authors declared no potential conflicts of interest with respect to the research, authorship, and publication of this article.

Funding

The authors received no financial support for the research, authorship, and publication of this article.

References

[1] Sposito, G., Gupta, V.K., Bhattacharya, R.N., Foundation Theories of Solute Transport in Porous Media: A Critical Review, *Adv. Water Res.*, 2, 1979, 59-68.
[2] van Genuchten, M.Th., Alves., W.J., Analytical Solutions of the One-Dimensional Convective-Dispersive Solute Transport Equation, *U.S. Department of Agriculture, Technical Bulletin*, 1661, 1982, 151.
[3] Latinopoulos, P., Tolikas, D., Mylopoulos, Y., Analytical Solutions for Two-Dimensional Chemical Transport in Aquifers, *J. Hydrol.*, 98, 1988, 11–19.
[4] Jaiswal, S., Chopra, M., Das, S., Numerical Solution of Two-Dimensional Solute Transport System Using Operational Matrices, *Trans. Por. Med.*, 122, 2018, 1-23.
[5] Aissa, M., Verstraete, T., Vuik, C., Toward a GPU-Aware Comparison of Explicit and Implicit CFD Simulations on Structured Meshes, *Comp. & Math. Appl.*, 74(1), 2017, 201-217.
[6] Brась, M., Cardone, A., Jackiewicz, Z., Pierzchała, P., Error Propagation for Implicit-Explicit General Linear Methods, *Appl. Num. Math.*, 131, 2018, 207-231.
[7] Franc, J., Horgue, P., Guibert, R., Debenest, G., Benchmark of Different CFL Conditions for IMPES, *Compt. Rend. Méca.*, 344(10), 2016, 715-724.
[8] El-Amin, M.F., Kou, J., Sun, S., Convergence Analysis of the Nonlinear Iterative Method for Two-Phase Flow in Porous Media Associated with Nanoparticle Injection, *Int. J. Num. Meth. Heat Fluid Flow*, 27, 2017, 2289-2317.
[9] Kou, J., Sun, S., A new treatment of capillarity to improve the stability of IMPES two-phase flow formulation, *Comp. & Fluids*, 39(10), 2010, 1923-1931.
[10] Redondo, C., Rubio, G., Valero, E., On the Efficiency of the IMPES Method for Two-Phase Flow Problems in Porous Media, *J. Petrol. Sc. Eng.*, 164, 2018, 427-436.
[11] Gwanghyun, J., Kwak, D.Y., An IMPES Scheme for a Two-Phase Flow in Heterogeneous Porous Media Using a Structured Grid, *Comp. Meth. App. Mech. Eng.*, 317, 2017, 684-701.
[12] Zhang, Y., Wan, D., Numerical Study of Interactions Between Waves and Free Rolling Body by IMPES Method, *Comp. & Fluids*, 155, 2017, 124-133.
[13] Martínez, V., A Numerical Technique for Applying Time Splitting Methods in Shallow Water Equations, *Comp. & Fluids*, 169, 2018, 285-295.
[14] El-Amin, M.F., Kou, J. Sun, S., Discrete-Fracture-Model of Multi-Scale Time-Splitting Two-Phase Flow Including Nanoparticles Transport in Fractured Porous Media, *J. Comp. App. Math.*, 333, 2018, 327-349.
[15] Alonso-Mallo, I., Portillo, A.M., Time Exponential Splitting Integrator for the Klein–Gordon Equation with Free Parameters in the Hagstrom-Warburton Absorbing Boundary Conditions, *J. Comp. App. Math.*, 333, 2018, 185-199.
[16] Arrarás, A., Portero, L., Improved Accuracy for Time-Splitting Methods for the Numerical Solution of Parabolic Equations, *Appl. Math. Comp.*, 267, 2015, 294-303.
[17] Bauzet, C., Time-Splitting Approximation of the Cauchy Problem for a Stochastic Conservation Law, *Math. Comp. Simu.*, 118, 2015, 73-86.
[18] Carichino, L., Guidoboni, G., Szopos, M., Energy-Based Operator Splitting Approach for the Time Discretization of Coupled Systems of Partial and Ordinary Differential Equations for Fluid Flows The Stokes Case, *J. Comp. Phy.*, 364, 2018, 235-256.
[19] Sun, S., Salama, A., El-Amin, M.F., Matrix-Oriented Implementation for the Numerical Solution of the Partial Differential Equations Governing Flows and Transport in Porous media, *Comp. & Fluids*, 68, 2012, 38-46.
[20] El-Amin, M.F., Kou, J., Sun, S., Salama, A., An Iterative Implicit Scheme for Nanoparticles Transport with Two-Phase Flow in Porous Media, *Procedia Computer Science*, 80, 2016, 1344-1353.
[21] Zhu, G., Li, A., Interfacial Dynamics with Soluble Surfactants: A Phase-Field Two-Phase Flow Model with Variable Densities, *Adv. Geo-Ener. Res.*, 4(1), 2020, 86-98.
[22] Zhang, S., Liu, Z., Shi, A., Wang, X. Development of Accurate Well Models for Numerical Reservoir Simulation, *Adv. Geo-Ener. Res.*, 3(3), 2019, 250-257.
[23] Millington, R.J., Quirk, Permeability of Porous Media, *Nature*, 183, 1959, 387-388.
[24] Lube, G., Breard, E.C.P., Esposti-Ongaro, T., Dufek, J., Brand, B., Multiphase Flow Behaviour and Hazard Prediction of Pyroclastic Density Currents, *Nature Rev Earth Environ*, 1, 2020, 348-365.
[25] El-Amin, M.F., Meftah, R., Salama, A., Sun, S., Numerical Treatment of Two-Phase Flow in Porous Media Including Specific Interfacial Area, *Procedia Computer Science*, 51, 2015, 1249-1258.
[26] El-Amin, M.F., Abbdel-Naeem, S., Numerical Algorithm for Unsteady Nonisothermal Two-Phase Flow in a Porous Cavity, *2020 International Conference on Intelligent Engineering and Management* (ICIEM), London, United Kingdom, 2020, 460-464.
[27] El-Amin, M.F., Kou, J., Sun, S., Numerical Investigation of Solute Transport in Fractured Porous Media Using the Discrete Fracture Model. *In: Krzhizhanovskaya V. et al. (eds) Computational Science – ICCS 2020, Lecture Notes in Computer Science*, Springer, Cham, 2020, 12143, 102-115.
[28] Walker, K.L., Homsy, G.M., Convection in a Porous Cavity, *J. Fluid Mech.*, 87, 1978, 449-474.
[29] Lauriate, G., Prasad, V., Natural Convection in a Vertical Porous Cavity: A numerical study for Brinkman-extended Darcy formulation, *J. Heat Transfer*, 109, 1987, 688-696.
[30] Bayatas, A.C., Pop, I., Free Convection in a Square Cavity using Thermal Non-Equilibrium Model, *Int. J. Therm. Sci.*, 41, 2002, 861-870.
[31] Saeid, N.H., Pop, I., Viscous Dissipation Effects on Free Convection in a Porous Cavity, *Int. Comm. Heat Mass Trans.*, 31, 2004, 723-732.
[32] Chamkha, A.J., Ismael, M.A., Conjugate Heat Transfer in a Porous Cavity Filled with Nanofluid and Heated by a Triangular Thick Wall, *Int. J. Therm. Sc.*, 67, 2013, 135-151.
[33] El-Amin, M.F., Khalid, U., Beroual, A., Magnetic Field Effect on a Ferromagnetic Fluid Flow and Heat Transfer in a Porous Cavity, *Energies*, 11(11), 2018, 3235.

ORCID iD

Mohamed F. El-Amin https://orcid.org/0000-0002-1099-2299
Shereen Abbdel-Naeem https://orcid.org/0000-0001-8605-0460

How to cite this article: El-Amin M.F., Abdel-Naeem, S.M. Multiscale Numerical Modeling of Solute Transport with Two-Phase Flow in a Porous Cavity, *J. Appl. Comput. Mech.*, 7(2), 2021, 396-403. https://doi.org/10.22055/JACM.2020.34734.2468